MECHANICAL BEHAVIOR OF ULTRAFINE-GRAINED Al–5Zn, Al–10Zn, Al–30Zn ALLOYS

E.V. Bobruk[1,2], X. Sauvage[3], N.A. Enikeev[1,2], B.B. Straumal[4,5] and R.Z. Valiev[1,2]

[1]Institute of Physics of Advanced Materials, Ufa State Aviation Technical University, 12 K. Marx str.,
Ufa 450000, Russia
[2] Laboratory for Mechanics of Bulk Nanostructured Materials, Saint Petersburg State University,
28 Universitetsky pr., Peterhof, Saint Petersburg, 198504, Russia
[3]Groupe de Physique des Materiaux, UMR CNRS 6634, Université et INSA de Rouen,
76801 Saint Etienne du Rouvray, France
[4] Laboratory of Hybrid Nanomaterials, National University of Science and Technology «MISIS»,
Leninskii prosp. 4, 119049 Moscow, Russia
[5]Institute of Solid State Physics, Russian Academy of Sciences, Ac. Ossipyn str. 2,
142432 Chernogolovka, Russia

Abstract. This work investigates the possibility of achieving superior ductility at room temperature (RT) in the binary Al-Zn alloys with different content of Zn from 5 to 30 wt.% thanks to the formation of ultrafine-grained (UFG) structures with a grain size below 500 nm by the high pressure torsion (HPT) techniques. The supersaturated solid solutions in investigated Al–Zn alloys decomposed during HPT processing resulting in nucleation and growth of secondary Zn precipitates and/or formation of grain boundary Zn segregations. The studied HPT deformed UFG Al-30Zn alloy demonstrates a ductility of 35%. The maximal elongation-to-failure was reached by applying a strain rate of 10^{-4} s^{-1}. The observed strain rate sensitivity values are close to ones typical of superplastic behavior and were usually observed only at high temperatures above 0.5 T_m. The UFG Al–30Zn alloy becomes superductile at RT. At the same time the ductility of UFG Al-5Zn, Al-10Zn alloys was found to be considerably lower and did not exceed 50% at RT. It is suggested that it is the Al-30Zn alloy that contains a volume fraction of Zn-wetted grain boundaries which is sufficient to provide active grain boundary sliding in an UFG material.

1. INTRODUCTION

Nowadays, there is a big interest in the development of to aluminum alloys with superplastic properties and creation of principally new shape forming processes, which are based on the superplastic (SP) deformation features. Superplasticity has certain advantages over other ways of shape forming in metals, which is due to the shape forming process itself and characteristics of the final microstructure. High deformability of alloys is the most evident advantage. It enables expanding the limits of usual shape forming techniques. Intensive plastic flow ensures much better shape reproduction in such complex items as discs and flanges, which allows reducing or totally excluding expensive mechanical treatment and decreasing the metal consumption [1-3]. The number of operations during metal processing should also reduce, as it will become possible to produce semi-items with shapes very much close to the sizes of finished items. Items with a definite shape in many cases can be produced via welding of separate parts. SP enables producing an item from one integral billet, which again reduces the cost and excludes loss of structural stability in weld seams. One of the advanced approaches for enhancing properties of aluminum alloys is refinement of their grain structure to the ultrafine-grained (UFG) state by such technique of severe plastic

Corresponding author: E.V. Bobruk, e-mail: e-bobruk@yandex.ru

deformation (SPD) as high pressure torsion (HPT) [3,4]. In recent work [5] high ductility values (δ = 160%) were achieved during room–temperature deformation of binary Al alloy Al–30 wt.% Zn, which is unusually high for the alloys of the Al-Zn system. It became possible to achieve such values due to the formation of an ultrafine–grained structure by SPD techniques. The UFG structure consists of Zn and Al phase grains and segregation of Zn on grain boundaries of the Al matrix. The authors have proposed that Zn segregations form due to enhanced diffusion in the near-the boundary area during HPT [6–11]. In [12] the authors also report about Zn particles inside grains and at triple joints in Al–2Zn, Al–10Zn, Al–30Zn alloys processed by HPT at room temperature. It is also shown that processing by HPT at 150 °C results in a significantly different structure with larger grains but smaller Zn particles [12].

The aim of the present study was to achieve high ductility in binary alloys Al–5Zn, Al–10Zn, Al–30Zn processed by HPT at room temperature. This work deals with peculiarities of a UFG structure produced by SPD, and its connection to mechanical properties in Al–5Zn, Al–10Zn, Al–30Zn alloys.

2. EXPERIMENTAL

Three binary alloys Al-5Zn, Al-10Zn, and Al-30Zn (wt.%) produced by half-continuous casting techniques were used for studies. Prior to high pressure torsion, initial billets were subjected to solid solution treatment for 1 h at 500 °C with subsequent water quenching to dissolve Zn in the aluminum matrix. Thermal-treated samples of the Al-Zn alloys with a diameter of 10 mm and a thickness of 1 mm were subjected to 10 rotations of HPT with 1 rpm rate at room temperature (RT) in order to form an UFG structure.

X-ray analyses were performed with the help of a Rigaku Ultima IV diffractometer. Cu $K_{\alpha 1}$ radiation (λ = 0.154060 nm) was used at a voltage of 45 kV and a current rate of 40 mA. The X-ray peaks were taken at a step of 0.01° and a dwell time of 2 sec. Monochromatization of a secondary peak was carried out using a parabolic graphite monochromator. The qualitative and quantitative phase analysis, lattice parameter estimation, quantitative evaluation of the coherent scattering domain (CSD) size D, crystalline lattice elastic distortion values $<\varepsilon^2>^{1/2}$ were performed using the MAUD software [13].

The Vickers hardness (HV) was measured using a Micromet–5101 microindentation tester with a load of 100 g for 15 s. In order to receive reliable results, each sample was measured more than 10 times.

Mechanical tensile tests of flat samples after HPT with a gauge part of 4.0×1.0×0.8 mm were performed at room temperature for Al–5Zn, Al–10Zn, Al–30Zn alloys and at 100 °C for Al–30Zn alloy on an Instron 8862 machine. The tensile tests were performed in the strain rate range 10^{-2} - 10^{-4} s^{-1}. The strain rate sensitivity coefficient was determined according to the formula [1-3]:

$$m = \frac{d\ln\sigma}{d\ln\varepsilon}.$$

The structural characterization by TEM was performed on a JEOL JEM 2100 electron microscope using dark and bright fields. The average grain size was calculated by measuring more than 250 grains. Z-contrast images were also recorded in HAADF STEM on a JEOL ARM 200F microscope.

Using a scanning electron microscope (SEM) JSM-6390, size and distribution of UFG Zn phases were analysed before and after the tensile test, as well as deformation relief of the surface previously polished to tensile specimens was investigated.

3. RESULTS AND DISCUSSION

3.1. Structure peculiarities of Al–5Zn, Al–10Zn, and Al–30Zn alloys after processing by HPT technique

Electron-microscopy studies demonstrate that during high pressure torsion a homogeneous ultrafine-grained (UFG) structure is formed in studied binary Al alloys Al–5Zn, Al–10Zn, and Al–30Zn. In [12] it is reported that during HPT grain structure refinement is accompanied with the decomposition of the Zn solid solution in fcc Al, leading to the nucleation of Zn particles. X-ray analysis supports these observations. Fig. 1 displays the intensity of X-ray peaks of Al phase and Zn phase after HPT. Fig. 2 presents the Al–5Zn structure after HPT. The grain size of the aluminum matrix after HPT is 500±45 nm, and the size of Zn precipitates in the Al matrix is 30±7 nm. Large particles of Zn with a size over 100 nm formed in triple joints of the grains. Some boundaries of aluminum grains are covered by Zn segregations. In the Al–10Zn alloy structure the grain size of the aluminum phase is 435±25 nm, the size of Zn precipitates in the Al matrix is 20±5 nm. Large particles of Zn with a size up to 200 nm form in triple joints of Al grains. Some boundaries of Al grains are covered with Zn segregations (Fig. 3). A volume fraction of such boundaries is not that high and consist about 20-30%. In the Al-30Zn alloy structure the grain size of the Al phase is 350±30 nm, the size of Zn
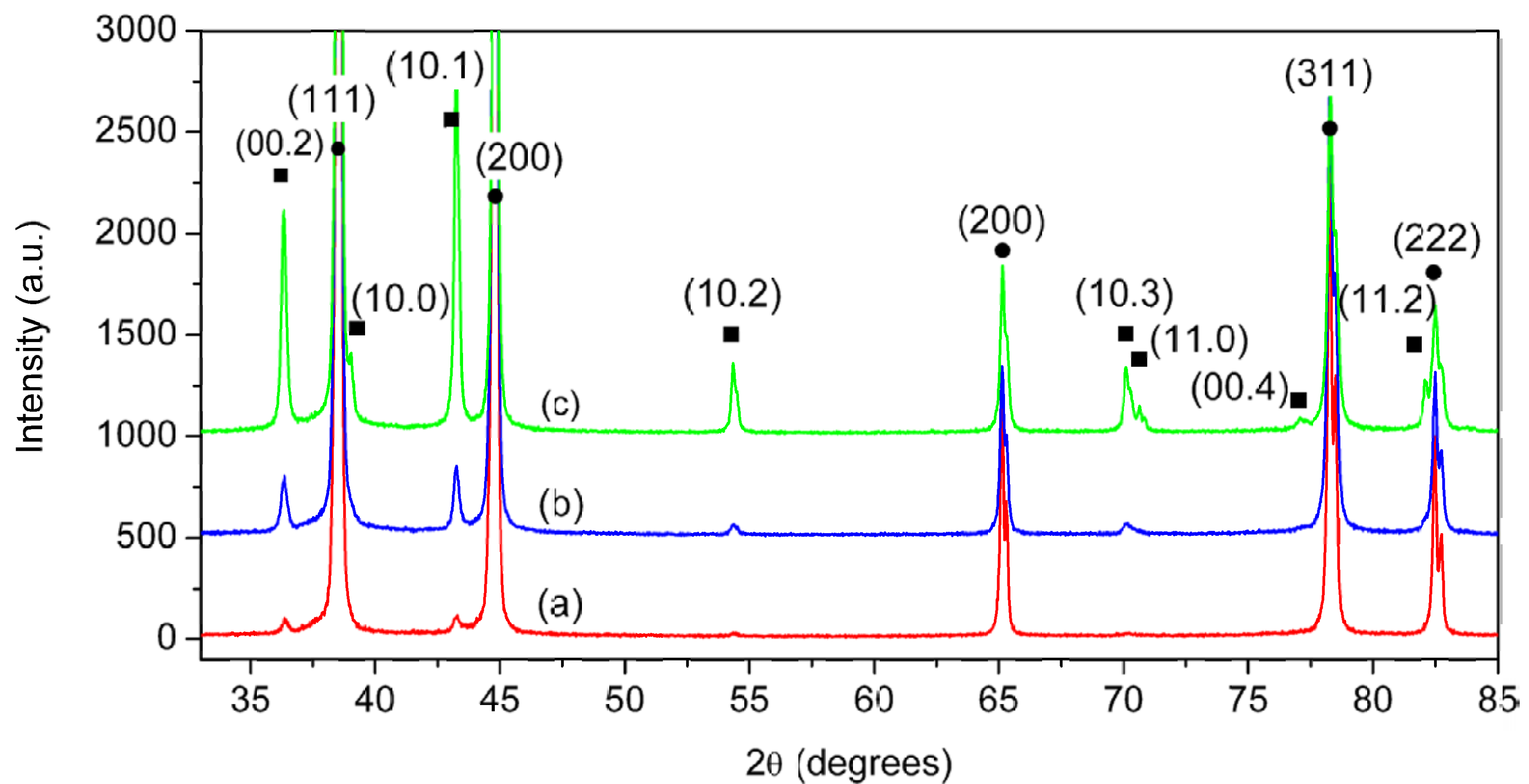
Fig. 1. Segments of X-ray patterns taken from Al alloys samples: (a) - Al–5Zn, (b) - Al–10Zn, (c) - Al–30Zn after HPT (● - Al; ■ - Zn).
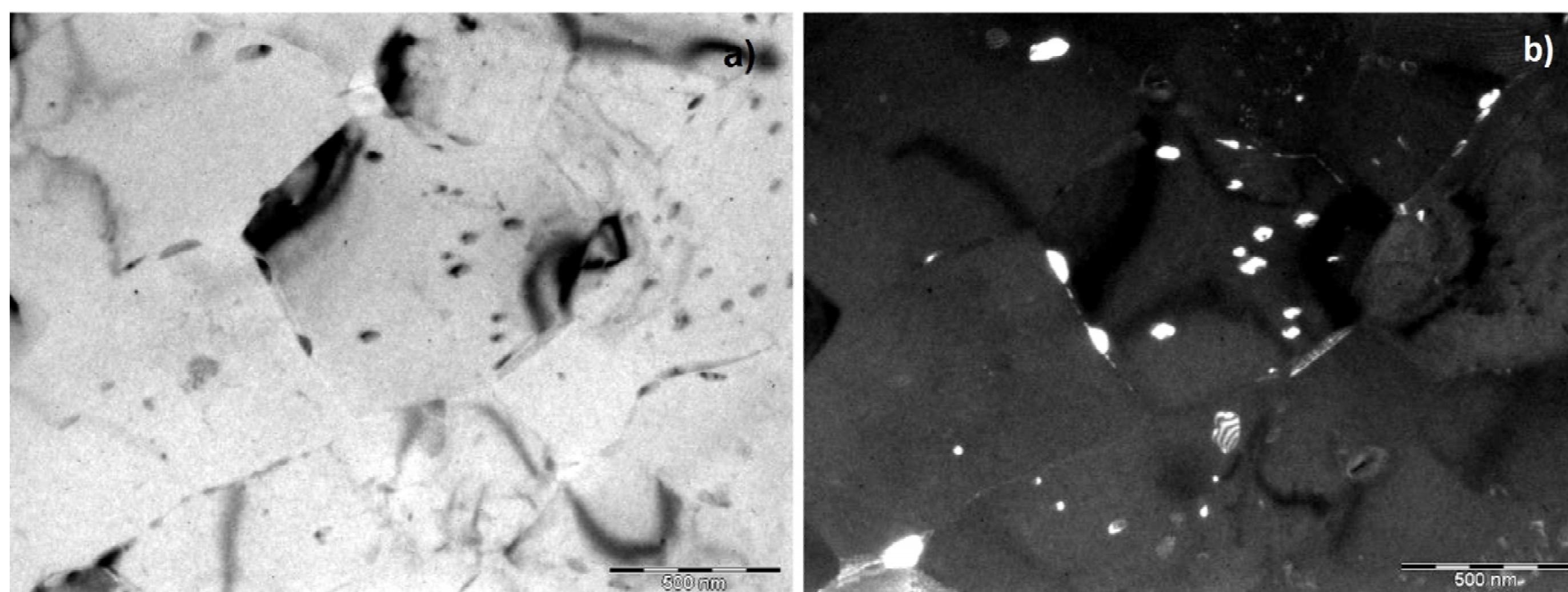
Fig. 2. UFG microstructure of Al–5Zn alloy after HPT: (a) - bright field TEM image; (b) - dark field TEM image.
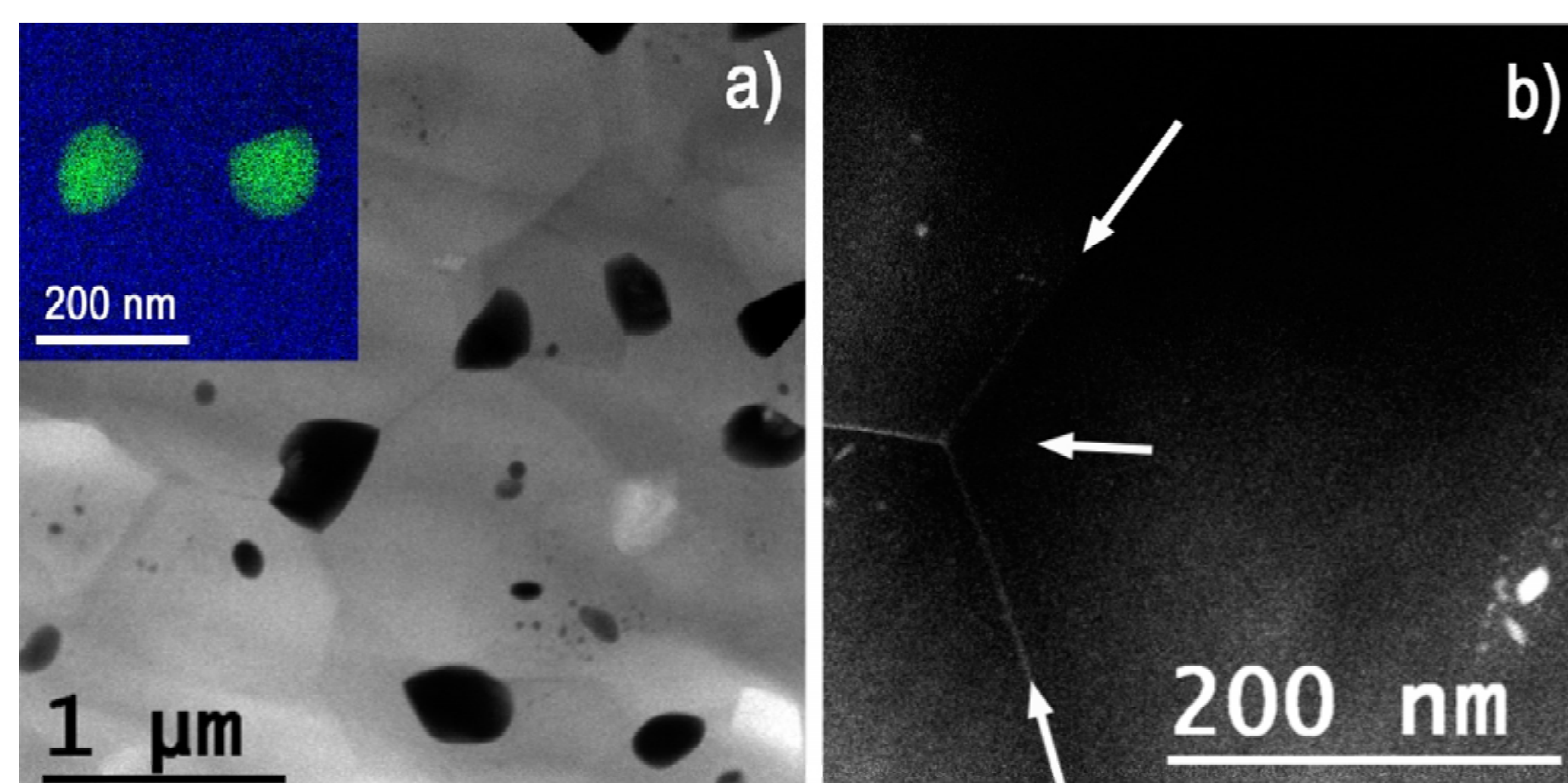
Fig. 3. UFG microstructure of Al–10Zn alloy after HPT: (a) - bright field STEM image and confirmed by the EDS map (inset, with Al-K blue and Zn-K green); (b) - dark field STEM image.

precipitates in the Al matrix is 10±4 nm. Large particles of Zn with a size over 200 nm form in triple joints of Al grains. Many boundaries of Al grains are also covered with segregations (Fig. 4). More detailed discussion of the Zn phase generation and growth can be found in our previous work [12]. Table 1 lists the volume fraction of Zn particles after HPT.

HPT of the Al–5Zn alloy results in an increase of the volume fraction of Zn from 0 to 0.78±0.05%. Higher Zn concentration in the Al–10Zn, Al–30Zn alloys leads to increase of the volume fraction of the Zn phase to 3.16±0.07%, and 16.4±0.3%, respectively. This fact demonstratess that HPT drives the mass transfer processes leading to intensive formation of
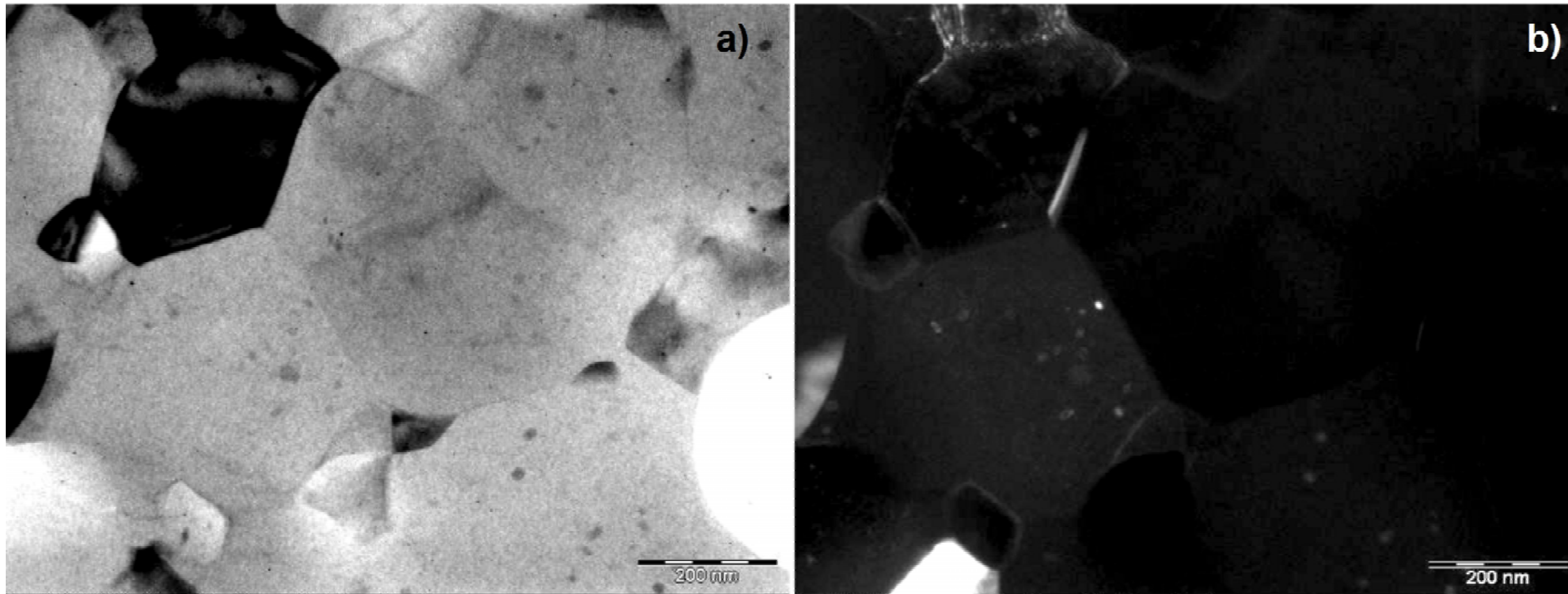
Fig. 4. UFG microstructure of Al–30Zn alloy after HPT: (a) - bright field TEM image; (b) - dark field TEM image.

Table 1. Microstructure parameters measured by X-ray analysis.

State	Volume fraction of Zn after HPT,%	Lattice parameter of Al after HPT, Å	CSD size of Al, nm	Microdistortions of Al lattice,%	Dislocation density,m^{-2}
UFGAl–5Zn	0 / 0.78±0.05	4.0499±0.0002	246±7	0.028±0.00025	$1.3 \cdot 10^{13}$
UFGAl–10Zn	0 / 3.16±0.07	4.0493±0.0001	186±5	0.0446±0.00024	$2.9 \cdot 10^{13}$
UFGAl–30Zn	0 / 16.4±0.03	4.0488±0.0001	159±4	0.0580±0.00028	$4.4 \cdot 10^{13}$

a new phase [6-11].The size of coherent scattering domains increases with the Zn content in the alloy, and the dislocation density grows noticeably for samples with a larger concentration of Zn. This observation can be accounted by the fact that an increase in the concentration of solute atoms in the solid solution promotes dislocation generation. The decomposition of the solid solution is also confirmed by a slight, change of the Al lattice parameter. It can be seen that in Al-10Zn and Al-30Zn alloys, solid solution treatment results in a reduction in the lattice parameter, as compared with pure Al, which is caused by Zn atoms in solid solution. This can be explained by the smaller atomic radius of Zn (138 nm) as compared to Al (143 nm) [14]. It is known that the dissolution of one atomic percent of Zn in Al leads to a decrease in the lattice parameter by 0.00075 Å [14]. In particular, HPT of Al–30Zn results in the lattice parameter change from 4.0439±0.0003 to 4.0488±0.0005 Å, whereas in the alloy Al–5Zn it reduces from 4.0504±0.0003 to 4.0499±0.0002, and in Al–10Zn from 4.0489±0.0003 to 4.0488±0.0001 Å. HPT processing leads to an increase in the lattice parameter, confirming the strain-induced decomposition of solid solution and the precipitation of Zn. Noteworthy, in the case of the Al-5%Zn alloy, after HPT the fcc Al phase is almost completely free of Zn, while for the two other alloys a certain amount of Zn still remains in the Al matrix.

3.2. Mechanical properties at RT of Al–5Zn, Al–10Zn, and Al–30Zn alloys after processing by HPT technique

The results of microhardness measurement in the initial state after quenching and HPT are listed in Table 2. The hardness of alloys after quenching (prior to HPT) increases with the increase of Zn concentration in the solid solution. After HPT processing at RT the hardness of all UFG alloys is rather similar, which can be explained by a similar grain size and a low amount of Zn in solid solution (Table 2). It also seems to indicate that there is a predominant solid solution hardening effect over the strengthening effect from grain structure refinement in these materials. The Zn particles also do not ensure additional significant strengthening, as their size and interparticle distance is large [9].

The mechanical tests were conducted at room temperature in the strain rate range from 10^{-2} to 10^{-4} s^{-1} to determine the parameter of strain rate

Table 2. Microhardness.

Material	H_v, Initial state	H_v, after HPT
Al–5Zn	62±3	78±2
Al–10Zn	101±5	84±3
Al–30Zn	156±5	81±3
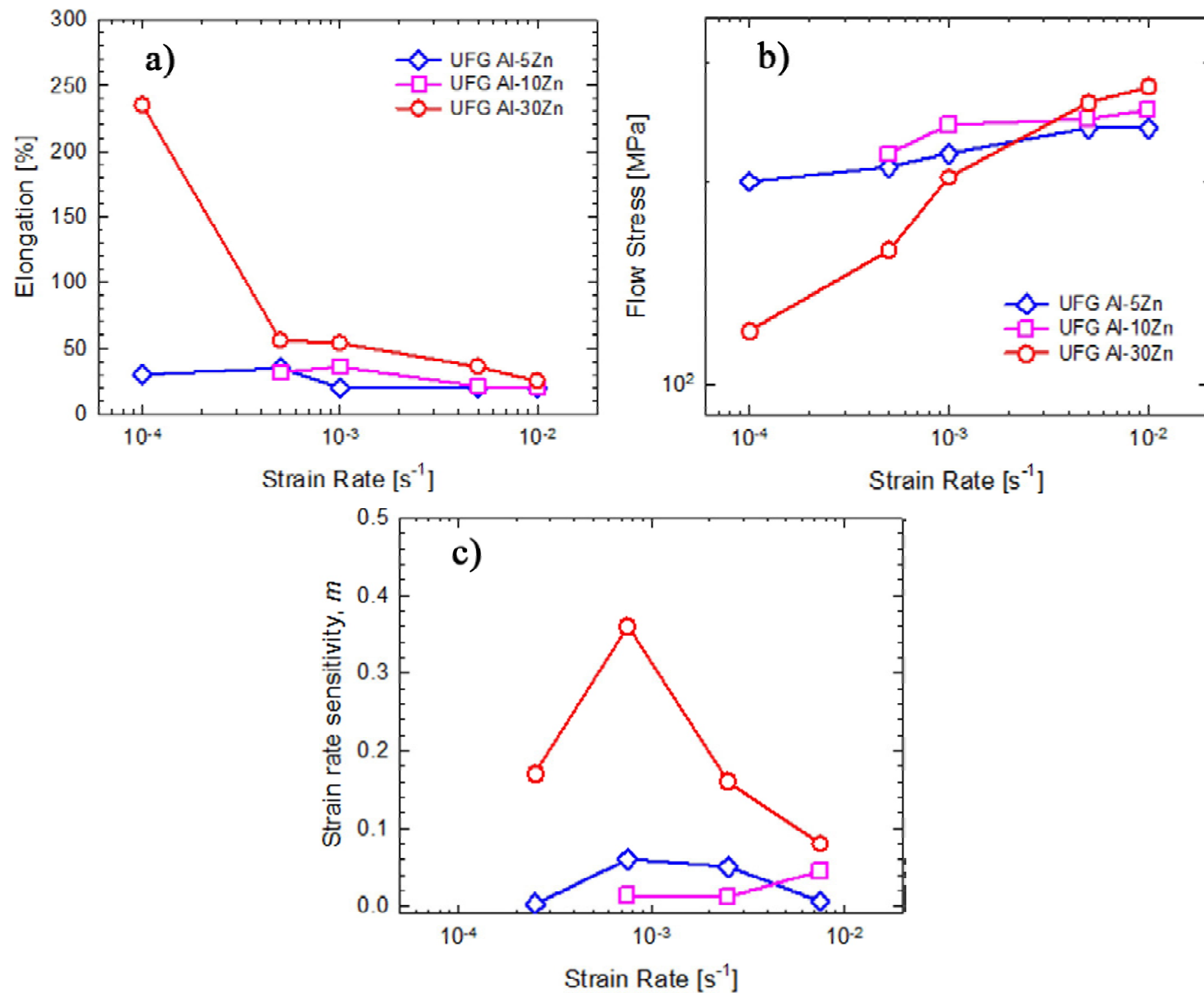
Fig. 5. Mechanical tensile tests of UFG samples of Al–5Zn, Al–10Zn, Al–30Zn alloys at RT: (a) - strain rate vs elongation to failure logarithmic dependence; (b) - flow stress vs strain rate logarithmic dependence; (c) - sensitivity coefficient (*m*) vs strain rate logarithmic dependence.
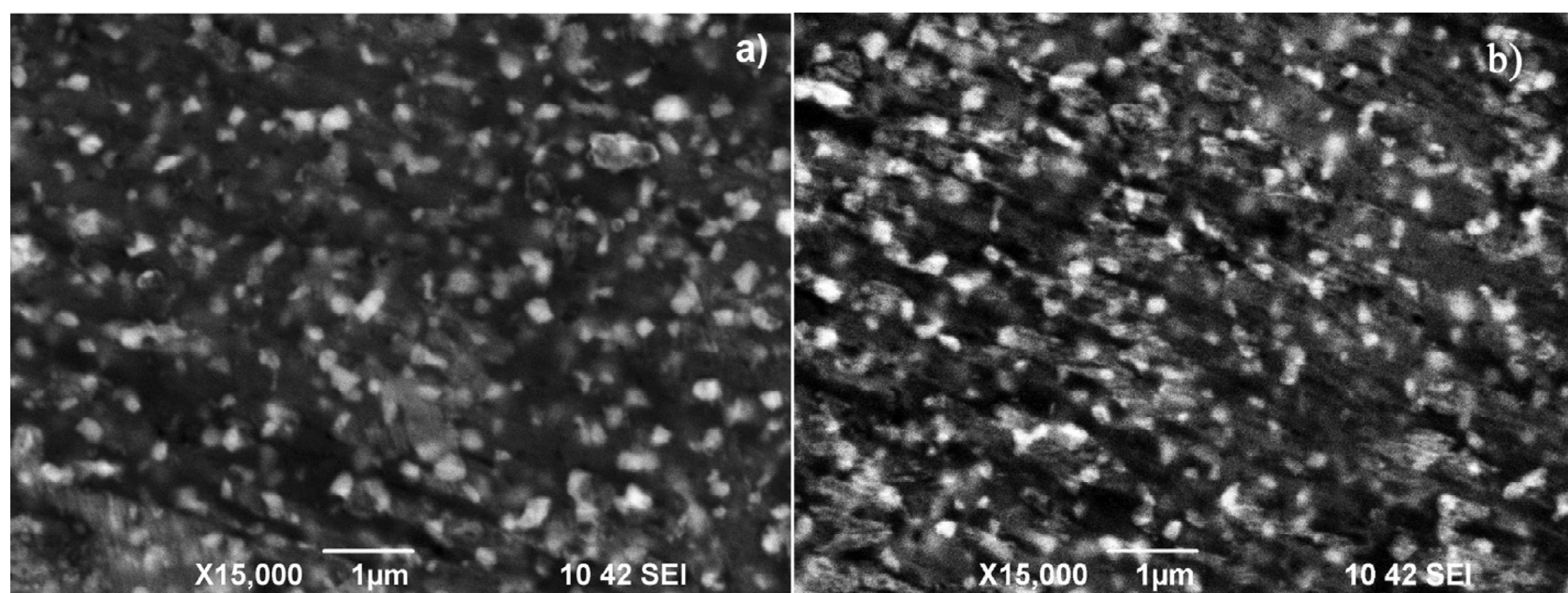
Fig. 6. Structure of UFG Al–30Zn alloy: (a) - before mechanical tensile tests; (b) - after mechanical tensile tests at RT (SEM).

sensitivity. Fig. 5 displays the strain-rate dependence of the flow stress, σ, during deformation, strain rate sensitivity coefficient, *m,* and elongation to failure.

After HPT the ultrafine-grained Al–30Zn alloy exhibits unusually high ductility at room temperature with a maximum elongation of 235 % when the strain rate is 10^{-4} s^{-1}. The strain-rate dependence of the maximum flow stress is shown in Fig. 5b , the values of the strain rate sensitivity are shown in Fig. 5c. It can be seen that the strain rate sensitivity for strain rates between $5 \cdot 10^{-3}$ and 10^{-4} s^{-1} is high and of the order of *m*=0.26. Such high values of m are close to those anticipated for a process such as

the viscous glide of dislocations, where *m*=0.33 [6]. However, this behaviour is observed only in the conditions of high temperature creep at temperatures above 0.5 T_m, where T_m is the melting temperature [6]. The grain boundary sliding during deformation plays an important role in the increase of the strain rate sensitivity coefficient and high ductility achievement in the ultrafine-grained Al–Zn alloys [1,2,6,11]. UFG Al-5Zn and Al-10Zn alloys do not demonstrate promoted ductility, its value does not exceed 50%. It is suggested that it is the Al-30Zn alloy that contains a volume fraction of Zn-wetted grain boundaries which is sufficient to provide active grain boundary sliding in an UFG material [12].
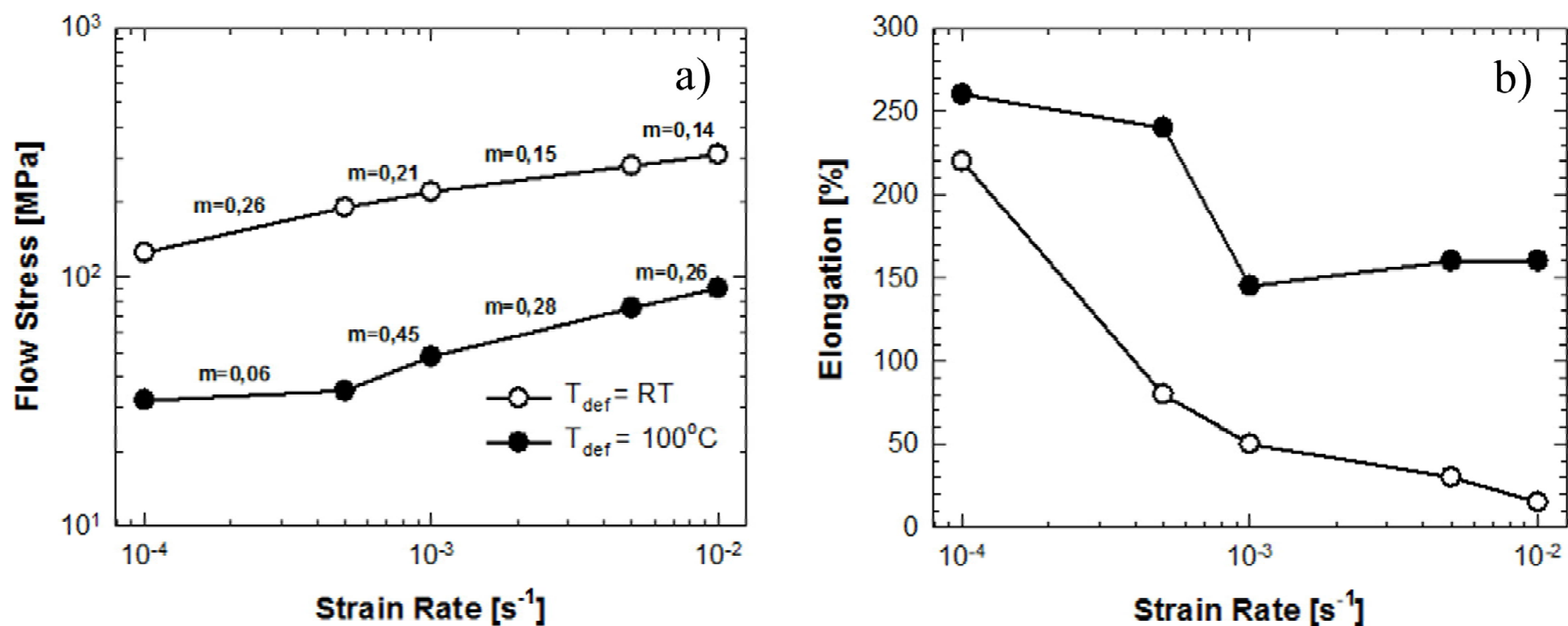
Fig. 7. Mechanical tensile tests of UFG samples of Al–30Zn alloy at RT (○) and at 100 °C (●): (a) - flow stress vs strain rate logarithmic dependence; (b) strain rate vs elongation to failure logarithmic dependence.
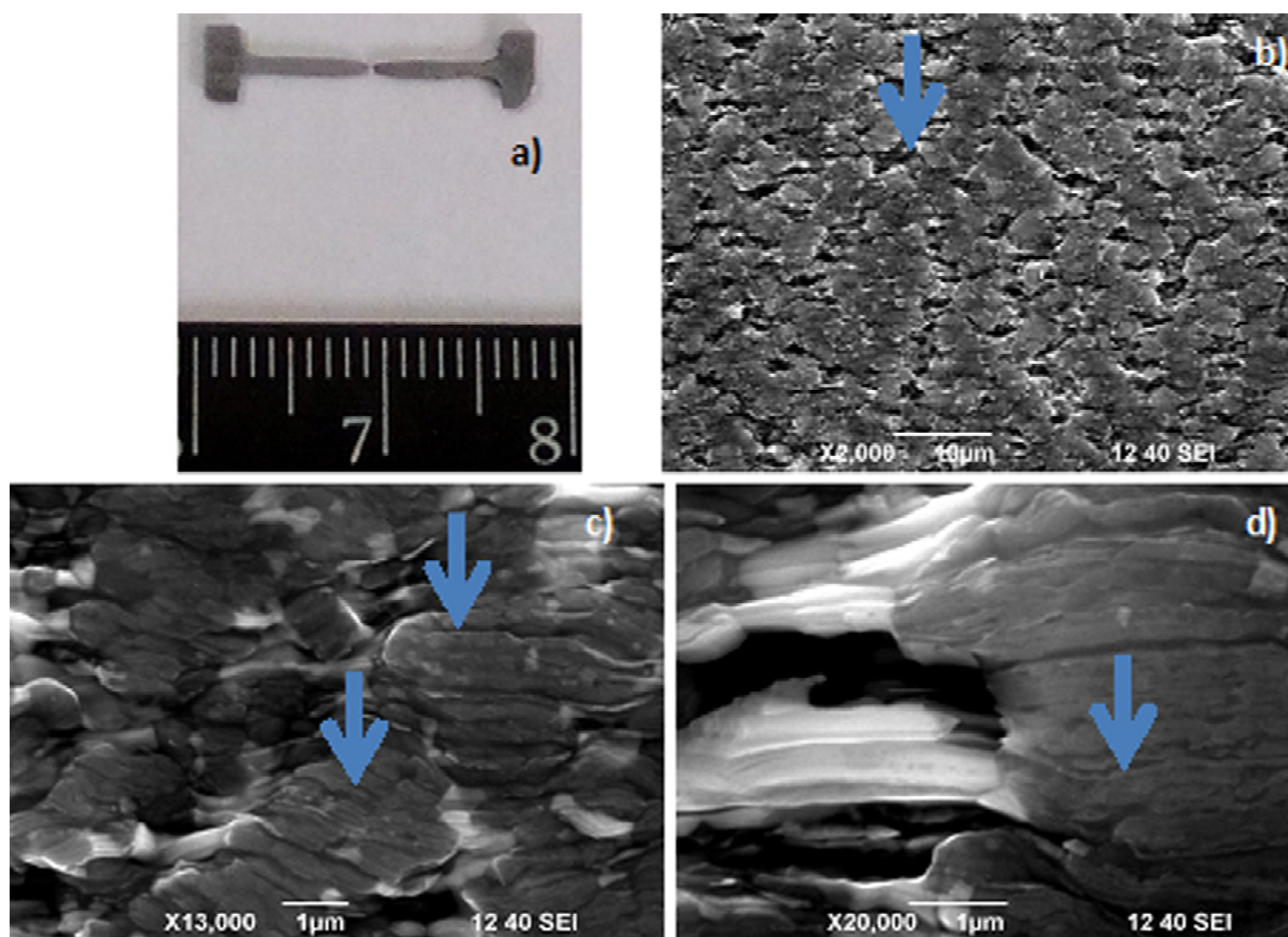
Fig. 8. (a) - sample view and (b, c, d) - deformation relief of the UFG Al–30Zn alloy after mechanical tensile tests at RT (SEM).

Fig. 6 displays the structure before and after mechanical tests at room temperature. It is important to note that there is no significant growth of Zn particles during deformation imposed by the mechanical tests at room temperature.

3.3. Mechanical properties of Al–30Zn alloy at RT and at 100 °C after processing by HPT technique

Fig. 7 presents the strain-degree dependence of the strain rate sensitivity coefficient of the binary alloy Al–30Zn during mechanical tensile tests at RT and at 100 °C. After HPT, the ultrafine-grained Al–30Zn alloy exhibits high ductility at 100°C with a maximum elongation of 265 %, when the strain rate is 10^{-4} s^{-1}. The strain-rate dependence of the maximum flow is shown in Fig. 7b , where the values of

the strain rate sensitivity, *m*, are also given. The strain-rate dependence of the maximum flow stress after mechanical tests at 100 °C is identical to the strain-rate dependence of the maximum flow stress after mechanical tests at RT. It can be seen that the strain rate sensitivity for strain rates between $5 \cdot 10^{-3}$ and 10^{-4} s^{-1} is high and of the order of *m*=0.45.

The scanning electron microscopy images of the samples after tension showed that necking did not take place during deformation, i.e. plastic flow localization was suppressed (Fig. 8a). The strain relief on the surface of processed samples represents single slip bands within the grains–intragranular slip (Figs. 8c and 8d). The strain localizes in the areas exceeding the grain size and leading to the formation of long shear bands, which in return results in the formation of a large number of microcracks (Fig. 8b). The UFG structure obtained by HPT with well

distributed Zn particles, and Zn segregations along Al grain boundaries lead to the features of SP at room temperature. Grain boundary dislocations and Zn rich layers obviously stimulate grain boundary sliding, providing high strain rate sensitivity and increased ductility [5-7].

4. CONCLUSIONS

1. During HPT an UFG structure forms in Al–5Zn, Al–10Zn, and Al–30Zn alloys, the grain size of Al and Zn phases decreases with the Zn concentration increase in the alloy. The decomposition of the supersaturated solid solution during HPT results in the nucleation of Zn particles inside Al grains and at triple joints and also to GB segregations. However, only UFG Al-30Zn alloy major part of interfaces contain Zn segregations. Judging by the X-ray analysis data, and as expected by the phase diagram, an increase of the Zn concentration in the alloy leads to enhancement of the volume fraction of the precipitated Zn as well.

2. The mechanical tensile tests at room temperature show that the Zn concentration increases from 5 to 30% results in the reduction of flow stress during deformation and the enhanced strain rate sensitivity. The studied Al–30Zn alloy demonstrates a superductility, which is unusually high for the room temperature state. The maximal elongation-to-failure reaches 235% at RT. The mechanical tensile tests at 100 °C show the maximal elongation-to-failure 265 % at a strain rate of 10^{-4} s^{-1}. The flow stress value increases monotonously with an increasing strain rate. These superplasticity features are related not only to UFG structure of Al-30Zn but also to formation of Zn segregations at grain boundaries which promote active grain boundary sliding and high strain rate sensitivity of the material's deformation.

ACKNOWLEDGEMENTS

REFERENCES

[1] O.A. Kaibyshev and F.Z. Utyashev, *Superplasticity, changes in the structure and processing of hard-alloy* (Nauka, Moscow, 2002).

[2] O.A. Kaibyshev, *Superplasticity of Alloys, Intermetallics, and Ceramics* (Springer-Verlag, Berlin, Germany, 1992).

[3] R.Z. Valiev, A.P. Zhilyaev and T.G. Langdon, *Bulk Nanostructured Materials: Fundamentals and Applications* (John Wiley & Sons, Inc., Hoboken, USA, 2014).

[4] R.Z. Valiev, Y. Estrin, Z. Horita, T.G. Langdon, M.J. Zehetbauer and Y.T. Zhu // *JOM* **58** (2006) 33.

[5] R.Z. Valiev, M.Yu. Murashkin, A. Kilmametov, B. Straumal, N.Q. Chinh and T.G. Langdon // *J Mater Sci* **45** (2010) 4718.

[6] N.Q. Chin, R.Z. Valiev, X. Sauvage, G. Varga, K. Havancsak, M. Kawasaki, B. Straumal and T. Langdon // *Advanced engineering materials* **16** (2014) 1000.

[7] R. Z. Valiev, M. Yu. Murashkin, A. Kilmametov, B. Straumal, N. Q. Chinh and T. G. Langdon // *J Mater Sci* **45** (2010) 4718.

[8] B. B. Straumal, X. Sauvage, B. Baretzky, A.A Mazilkin and R. Z. Valiev // *Scripta Materialia* **70** (2014) 59.

[9] A.A Mazilkin, B. B. Straumal, E. Rabkin, B. Baretzky, S. Enders, S.G. Protasova, O.A. Kogtenkova and R. Z. Valiev // *Acta Materialia* **54** (2006) 3933.

[10] A.A Mazilkin, B. B. Straumal, M.V. Borodachenkova, R. Z. Valiev, O.A. Kogtenkova and B. Baretzky // *Materials letters* **84** (2012) 63.

[11] N.Q. Chin, T. Csanadi, T. Gyori, R.Z. Valiev, B. Straumal, M. Kawasaki and T. Langdon // *Materials Science and Engineering A* **543** (2012) 117.

[12] X. Sauvage, M.Yu. Murashkin, B.B. Straumal, E. Bobruk and R. Z. Valiev // *Advanced engineering materials*, DOI: 10.1002/adem.201500151, (2015).

[13] L. Lutterotti, S. Matthies and H.-R. Wenk, In: *Proceeding of the Twelfth International Conference on Textures of Materials (ICOTOM-12)* **1** (1999) 1599.

[14] J. E. Hatch, *Aluminum: Properties and physical metallurgy* (American society for metals, Metals Park, Ohio, 1984).